Suppressing Flame over Electrical Wire in Confined Space by Oscillatory Airflow

Jinglong Lyu[1] (吕敬龙), Jinxin Zhang[1] (章金鑫), Xiaoming Gao[1] (高晓明), Caiyi Xiong[1,*] (熊才溢),

Xinyan Huang[2,*] (黄鑫炎)

[1] *School of Mechanical and Automotive Engineering, South China University of Technology, Guangzhou, China*

[2] *Department of Building Environment and Energy Engineering, The Hong Kong Polytechnic University, Hong Kong*

* Corresponding to ycxiong@scut.edu.cn (C. Xiong), xy.huang@polyu.edu.hk (X. Huang)

Abstract

Electric wires installed in confined spaces such as underground tunnels and false ceilings represent a prevalent source of fire occurrences. Such a hidden fire is hard to extinguish by traditional firefighting techniques. This paper proposes using oscillatory airflow for suppressing wire fire hazards in confined environments. A horizontal wire with polyethylene insulation and copper core is selected as the target, combined with an electromagnetic piston developed to generate airflows oscillating at frequencies from 50-70 Hz and velocities up to 0.28 m/s. Results confirm that, compared to steady wind, oscillatory airflow can achieve extinction at a lower velocity while consuming less electricity power. The heat transfer involving oscillatory flows between the flame and the fuel is analyzed, revealing that augmented fuel cooling and diminished flame radiation are the primary contributors to its improved extinguishing performance. Unsteady flame stretch under oscillatory airflow is also analyzed, providing mechanistic explanation for the superior extinction performance observed for lower-frequency flows. An extinction criterion based on fuel heat loss and airflow perturbation is formulated to explain the extinction limits. This work introduces a low-carbon firefighting technique that employs normal air as extinguishing agent, and it helps expand the channel for fire safety design in constrained environments.

Keywords: *Electrical wire; Blow-off; Oscillatory airflow; Extinguisher; Firefighting*

Nomenclature

Symbols			
A	cross-section area (m^2)	λ	conductivity ($W/m^{-}K$)
a	flame strain rate (s^{-1})	ω	angular frequency (s^{-1})
c	specific heat ($J/kg{\cdot}K$)	γ	kinematic viscosity (m^2/s)
C	fitting constant	ϵ	reflection ratio
D	diffusion coefficient (m^2/s)	ψ	flame-extinguishment energy index
		φ	oscillation amplitude (m)

d	diameter (m)	ε	emissivity
E	Energy consumption (J)	σ	Stefan-Boltzmann constant ($W/m^2 \cdot K^4$)
f	frequency (s^{-1})	β	volume expansion coefficient (K^{-1})
G	perimeter (m)	δ	thickness (m)
Gr	Grashof number	Θ	heat loss factor
g	gravity acceleration (m/s^2)	***Subscripts***	
ΔH	latent heat (kJ/kg)	∞	ambient
h	convection heat transfer coefficient	ba	bare core
	($W/m^2 \cdot K$)	br	burnout
L	length (m)	c	metal core of electrical wire
Nu	Nusselt number	D	diffusion
P	pressure (Pa)	ex	extinction
Pr	Prandtl number	F	forced convection
$\dot{Q}$	heat transfer (W)	f	flame
R	resistance (Ω)	g	gas phase
Re	Reynolds number	m	buoyancy and oscillatory-mixed flow
r	radius (m)	N	natural convection
T	temperature (K)	o	oscillatory airflow
t	time (s)	p	piston-based oscillatory flow generator
U	velocity (m/s)	py	pyrolysis
V	voltage (V)	r	radiation
E	energy consumption (J)	s	polyethylene layer of electrical wire
Greek		w	wind
ρ	density (kg/m^3)		

I. Introduction

Electrical wiring systems play a critical role in urban power transmission infrastructure, however, their susceptibility to accidental overheating and short-circuiting poses an escalating fire risk in densely populated areas [1,2]. In general, urban cables are frequently installed in confined spaces, including suspended ceiling, cable tray, underground tunnel [3–5], and vertical well. In such environments, traditional fire suppression agents like chemical powder, water mist, and inert gas are difficult to store nearby and challenging to contact and suppress the flame over the wire. Consequently, the development of improved wire fire mitigation strategies tailored to constrained settings holds both scientific importance and practical value.

Within confined environments, ambient air represents the most easily accessible medium. As combustion fundamentally constitutes a gas-phase reaction, variations in airflow dynamics directly influence flame behavior and stability. Over recent decades, extensive research has systematically

characterized the interaction between airflow and electrical wire fires [6], elucidating the effects of environmental factors such as airflow velocity [7–9], orientation [7–12], oxygen [13], temperature [14,15], and pressure [10]. Based on the relative direction of airflow, wire fire spreads are classified into three modes: opposed [10], concurrent [8], and transverse [7] configurations. Notably, under all conditions, wire fire extinction occurs when airflow velocity exceeds a certain value. Such an air-induced extinction can be explained from two aspects: 1) in the gas phase flame-sheet, the residence time of combustible species becomes smaller than its chemical time required for continuous burning [8,16], and 2) in the fuel-flame-supply cycle, the reduced heat feedback from flame can no longer maintain fuel pyrolysis [6,9]. In general, experimental evidence confirms that ambient air serves as an eco-friendly, effective, and readily applicable medium for mitigating wire fire hazards under constrained conditions.

However, using normal airflow for wire fire suppression is not easy. This is because, on the one hand, the air velocity required for critical extinction can be very large; for example, concurrent airflow exceeding 1.8 m/s is required to quench flames propagating along a horizontal 2 mm diameter wire [8], while opposed airflow of 1.1 m/s is needed for a 9-mm vertical wire fire [15], and on the other hand, deploying active airflow devices like pumps, fans, or blowers within confined spaces demands unobstructed air intake. This creates operational challenges in these constrained installations, where sidewall obstruction and heat accumulation effects can impede continuous airflow replenishment. Nevertheless, air remains an easily accessible medium with great firefighting potential. One may expect an enhanced suppression efficacy of air within confined space by optimizing its flow pattern.

Oscillatory airflow, a unique flow regime characterized by a dominant mean velocity component superimposed with periodic fluctuations, has found extensive applications in diverse industrial devices. Unlike steady airflow, oscillating flow propagates at discrete frequencies and phase velocities without requiring continuous external air supply. Over recent decades, this flow pattern has attracted significant attention for augmenting heat transfer in metallurgy process, thermoacoustic engines, and electronic components [17–19]. There are also existing works that have achieved flame extinctions in small-scale combustors through nozzle-induced oscillatory flows [20–22]. Studies involving a variety of heat transfer interfaces and temperatures have consistently demonstrated superior heat exchange performance under oscillatory flow conditions [19,23–25]. Mechanistically, this enhancement arises from energy transfer dynamics between the oscillating fluid and solid interface, modelled as time-averaged heat transport [23,24]. A critical factor in this process is the synergistic interaction among the bulk mean flow, fluctuating velocity perturbations, and buoyancy-driven flows induced by surface heat release. This multiscale interaction becomes particular influential for high-temperature objects engulfed in flames, where oscillatory and buoyant flows may collectively dominate convective heating and cooling [19,23]. Therefore, using oscillating airflow for cooling burning wires and arresting flame spread presents a promising solution. If available, such suppression could theoretically be achieved using simple oscillating devices (e.g., vibrating diaphragms) within confined spaces, eliminating need for large-scale air supply systems.

This work is therefore carried out, which aims to experimentally investigate the application of

oscillatory airflow for extinguishing wire fire and mitigating wire hazards in confined environments. Flame spread characteristics in both free and confined spaces are examined, with particular emphasis on analyzing heat transfer and critical flame behavior prior to extinction. A flame spread model incorporating oscillatory heat transfer dynamics is developed to elucidate the dominant heat transfer process during suppression. Besides, a theoretical criterion integrating wire heat loss and airflow perturbation is formulated to define critical extinction.

II. Experimental set-up

Figure 1a shows the experimental design. A vibrating system, comprising a signal generator (UTG9005C-II), an amplifier (CROWN T5), and a tube-like piston device, is utilized to induce oscillations in its front air. The generator produces a controllable sinusoid signal, which also controls the oscillating frequency. The amplifier then enhances the signal amplitude and determines the oscillating velocity. Finally, the amplified signal passes through the winding of electromagnet, causing its core to periodically attract and release an armature-mounted piston and converting the signal into mechanical vibration.

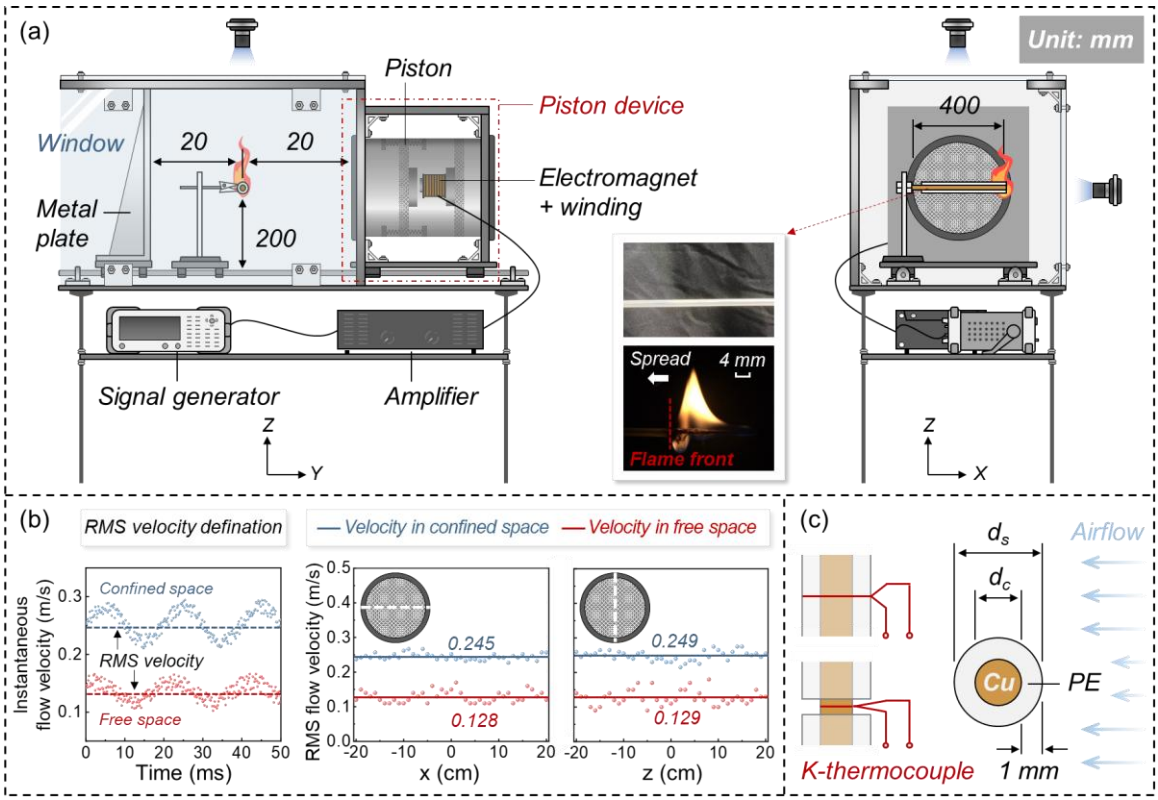

Fig. 1. (a) Experimental setup; (b) distribution of RMS velocity for a 50-Hz airflow in front of the piston system, and (c) wire configuration and thermocouple installation.

This electromagnet piston then serves as the source for generating the target oscillatory airflow. The piston diameter is 400 mm, which can create a uniform flow field of the same size, as evidenced by the root-mean-square (RMS velocity, defined as the average of instantaneous velocity) velocity

measurements along the horizontal centerline immediately in front of the piston [Fig. 1b]. This large piston ensures that arbitrary flame spreading along the wire experiences a uniform flow field, thereby enhancing the repeatability of the experiments. The system is designed to oscillate air at a frequency band of 50-70 Hz, which has been revealed to exhibit optimal heat transfer efficiency relative to system power consumption [26]. Also, such a frequency band is slightly above the piston resonant frequency (~ 35 Hz), so as to ensure safe operations.

To mimic a confined environment, a 400 mm side-length mental duct made of heat-resistant glass is designed and positioned in front of the piston face to channel the oscillatory airflow. The far end of the duct is sealed with a metal plate, which can reflect the airflow and leave enough space for wire burning. Both the piston and duct are affixed to the same horizontal slide [Fig. 1a], enabling precise positioning relative to the fire source. As an initial attempt, the horizontal confinement gap is fixed at 40 mm, so to prioritize investigations into the wire fire behaviors under constrained conditions. Such configuration mimics a safe region to shield wire fire hazards in confined spaces and causes a nearly double increase in RMS oscillatory velocity compared to free-space conditions, as measured in Fig. 1b.

The target wire fire adopts a standard configuration [2], consisting of a thin polyethylene (PE) tube of 100 mm long with a copper (Cu) core inserted. The Cu core diameter (d_c) is 2 mm, and the PE insulation thickness is 1 mm, see Fig. 1c. Key thermal properties of the wire are given in Table 1. During experiments, the wire is horizontally positioned within the test section at a height of 200 mm, aligned with the piston centerline and maintained 20 mm upstream from the duct inlet. This placement ensures stable flame propagation and prevents molten PE attachment, thereby ensuring experiment repeatability.

Table 1. Properties of wire materials and surrounding air

Property	Copper (Cu)	Polythene (PE)	Air
Density, ρ [kg/m^3]	8880	920	0.47
Heat capacity, c [J/kg-K]	385	2150	1070
Conductivity, λ [W/m-K]	400	0.33	5.39×10^{-2}
Pyrolysis temperature, T_{py} [K]	—	660	—
Pyrolysis latent heat, ΔH_{py} [J/kg]	—	2.54×10^{5}	—
Kinematic viscosity, γ [m^2/s]	—	—	76.4×10^{-6}

Before experiment, two K-type thermocouples (0.5 mm diameter, Omega XS-K-24) are placed at the wire center along its length direction, with one embedded within the copper core and the other affixed to the PE insulation surface, as shown in Fig. 1c. Temperature data are recorded by a multi-channel data acquisition system (HIOKI LR8431). A propane torch is used to ignite the wire from its right end. Upon flame stabilization and propagation close to the duct center, the piston system is activated, delivering oscillatory airflow towards the flame in the transverse direction. Once extinction occurs, a hot-wire anemometer (± 0.01 m/s, testo505i) is used to measure the pure oscillatory airflow

velocity at the flame position. The unstable flame behavior during extinction is monitored by two high-speed cameras (1,000 fps, SONY DSC-RX10M4) from the top and side views. The recorded videos are then converted into time-sequence images, which are then post-processed to determine the instantaneous flame front position. By calculating the first-order derivative of flame front location with respect to time, the flame spread rate (FSR) can be obtained. During experiments, each trial is repeated at least three times to reduce measuring error.

III. Result and discussion

A. Flame response behavior

The impact of space constraint on wire burning is first checked. Fig. 2a compares the spread of wire fire in open space with that in confined space. Initially, the piston system is not activated, allowing all wires to burn and develop freely without any external airflow. The most prominent feature in Fig. 2a is the remarkable similarity in flame shape, size, color, and spread rate (FSR), irrespective of whether in open or confined conditions. This implies that the confinement gap will not significantly affect the wire burning dynamics including its oxygen consumption, thermal feedback, and fuel pyrolysis. Fig. 2a also shows that the wire fire in confined space still undergoes three typical stages: an initial development spanning the beginning 2-cm, followed by a stable spread over the middle 6-cm, and decays at the next 2-cm wire end. To ensure reproducibility, only the stable flame spread at the middle 6-cm will be taken as the extinguishing target.

The piston is then activated, which first produces a 0.13-m/s airflow oscillating at a frequency of 50-Hz in open space (without the duct). Flame response behaviors are depicted in Fig. 2b. It can be seen that under the single impact of oscillatory airflow, the flame starts to oscillate along the streaming direction and transitions its combustion mode from steady propagation to fragmented flickering. Measurement further indicates a 35% reduction in the average flame spread rate compared to quiescent conditions, which can be attributed to the enhanced cooling effects caused by oscillatory airflow [19,26].

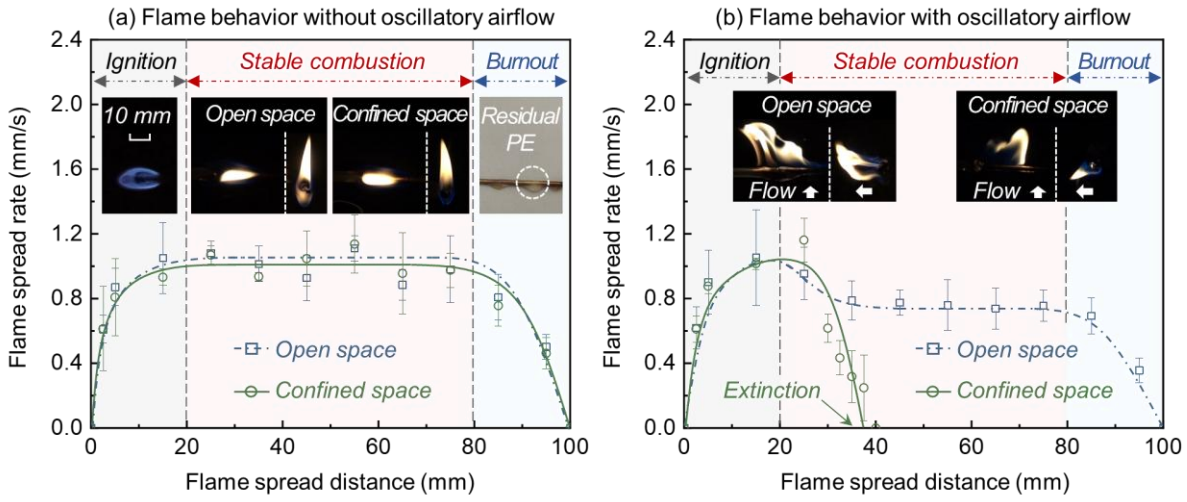

Fig. 2. Flame spread rate over electrical wire (a) without and (b) with oscillatory airflow.

However, if the piston working parameters (i.e., piston oscillation frequency and amplitude) are kept unchanged and the above test is solely repeated within the confined duct, rapid extinction can be observed as the flame enters the oscillatory field, see Fig. 2b. Specifically, the flame can be blown out in a short period of less than 20 s under the impact of reflected airflow, confirming the enhanced suppression efficiency of oscillatory airflow in confined spaces. Due to the influence of sidewall reflection, a prolonged displacement of flame from the wire surface and intensified flame fragmentation can be observed. Velocity measurements further indicate nearly a twofold increase in RMS oscillatory velocity (from 0.13 to 0.25 m/s) compared to open conditions, which is likely the primary factor contributing to flame extinction.

B. Critical extinction

To validate the generality of the observed extinction phenomenon across different oscillatory conditions, parametric studies are conducted spanning airflow velocities up to 0.30 m/s and frequencies from 50-70 Hz. Fig. 3 depicts the flame spread rate as a function of oscillatory airflow velocity at discrete frequencies. The results reveal a non-linear relationship characterized by two regimes: 1) at airflow velocity below about 0.05 m/s, flame spread rate exhibits a positive correlation with airflow velocity, attributed to enhanced oxygen transport to the reaction zone and thereby promoting wire burning; and 2) beyond this threshold, further velocity increases lead to a sharp decay in flame spread rate, and extinction occurs before complete flame arrest, demonstrating that the flame-fuel-supply cycle is significantly disrupted by the enhanced airflow perturbation. Notably, the critical extinction velocities under all oscillatory conditions (0.26 ± 0.02 m/s) are much lower than the blow-off velocity for normal wind (~0.50 m/s).

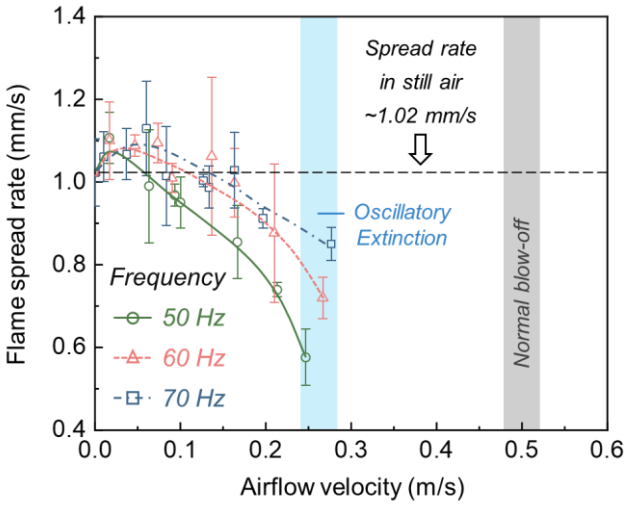

Fig. 3. Response of flame spread rate on wire to oscillatory airflow velocity at different frequencies.

Another feature observed in Fig. 3 is that the lower the frequency used, the lower the velocity required for oscillatory airflow to cause extinction. This implies that the superior efficacy of oscillatory airflow in fire suppression is not solely attributed to enhanced convective cooling, but may also be

associated with frequency-dependent mechanisms, e.g., the increased heat loss and reduced thermal feedback due to airflow-driven flame displacement. A detailed explanation will be given later.

To gain deeper insight into the extinguishing performance of oscillatory airflow, the extinction velocity ($U_{o,ex}$) is measured at a finer frequency interval of 5 Hz and is shown in Fig. 4. As seen, $U_{o,ex}$ exhibits a positive correlation with the airflow oscillating frequency, further validating the superior suppressing efficiency of low-frequency flow. However, when the confined duct is removed in these cases, extinction does not occur, and instead, the wire flame persists with unrestricted propagation. The removal of confined duct will also lead to the decrease of airflow velocity to a moderate value ($U_{o,open}$), see Fig. 4. This velocity attenuation, attributed to the effect of sidewall reflection, can be quantified by a ratio $\epsilon = U_{o,ex}/U_{o,open}$. Notably, ϵ is theoretically determined by the geometric characteristics of the confined space, as the oscillatory airflow propagating within the duct resembles a standing wave. In this work, an average of ϵ is measured to be 1.7 across the target frequency band. Details of how critical extinction is influenced by ϵ will be the subject of future study.

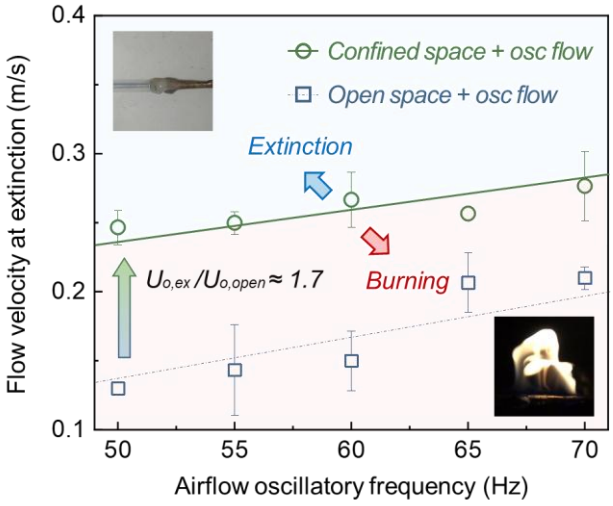

Fig. 4. Dependence of critical extinction flow velocity on air oscillating frequency.

C. Extinguishing power efficiency

To quantitively evaluate the technical advantages of oscillatory airflow relative to normal wind in fire suppression applications, an extinguishing index (ψ) is proposed, defined as the ratio of electrical energy consumption between the piston system (E_o) and a geometrically identical fan system (E_w) under equivalent extinction airflow velocity conditions:

$$\psi = \frac{E_o}{E_w} \tag{1}$$

here, both E_o and E_t can be calculated by the device working voltage (V), internal resistance (R), and extinction duration (t, defined as the duration from when the flame starts being deflected until extinction; for oscillatory airflow, t is 20-50 ms; for normal wind, t is 90-110 s), i.e., $E_o = (V_o^2/R_o)t_o$ and $E_w = (V_w^2/R_w)t_w$. For conditions where $\psi < 1$, using oscillatory airflow for fire extinguishing is more

energy-efficient. Conversely, the typical blow-off method by fan system is preferable.

Solutions of Eq. (1) at different frequencies from 50-70 Hz are plotted in Fig. 5. As a comparison, both the results obtained in confined duct and open space are presented. It can be seen that in most cases, ψ remains significantly below 1.0, except when airflows oscillating at frequencies exceeding 60 Hz are used for fire suppression in open-space conditions. It is also found that the lower the oscillatory frequency employed, the lower the energy consumption required for extinction. This can be attributed to two factors: 1) the extinction velocity of lower-frequency airflow is relatively smaller ($U_{o,ex}$ in Fig. 4), thereby requiring a smaller voltage (V_o) for generating such airflow; and 2) due to the frequency response characteristics of the electromagnetic piston [27], its resistance (R_o) increases as the working frequency decreases to resonant frequency (35 Hz). Also, operating the electromagnetic piston at frequencies below 35 Hz would further reduce energy consumption for suppression, however, short circuits may occur due to the sharp decrease in piston impedance to zero. Therefore, for the current electromagnetic piston, the low-frequency range of 50–70 Hz can serve as the optimal band for suppressing flames over electrical wires and mitigating fire hazards in confined spaces.

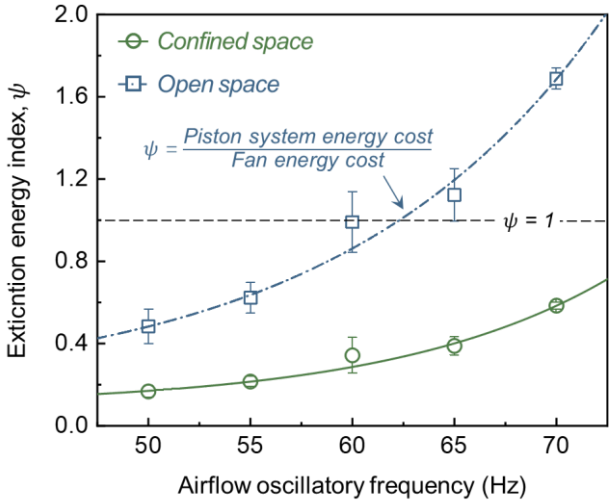

Fig. 5. Energy consumption ratio of oscillatory piston compared to fan system at extinction limits.

So far, all observations have demonstrated that, despite only differing in flow field structure, oscillatory airflow and normal wind exhibit a significant difference in the efficiency of inducing extinction. Hence, a comparative analysis of flame-fuel heat transfer under both flow conditions is necessary. Before this, the oscillation-induced heat transfer boundary must be examined first.

D. Oscillation-induced airflow boundary

In the work by Schlichting [28], the flow boundary of a circular cylinder subjected to transverse oscillating airflow has been analyzed in detail. In their work, experiments were carried out on a heated cylinder vibrating transversely in still air, with a focus on the heat transfer mechanism, particularly the heat convection, induced by oscillatory motion. Subsequent studies [19,23] extended this framework to

investigate the combined effects of oscillatory and buoyancy-driven flow on cylindrical convection. As seen, these foundational works share conceptual parallels with the present study, where a burning wire is exposed to transverse oscillatory airflow for fire suppression. Therefore, a similar analysis following [28] is adopted here to characterize the thermal boundary layer dynamics around the burning wire under oscillatory flow conditions.

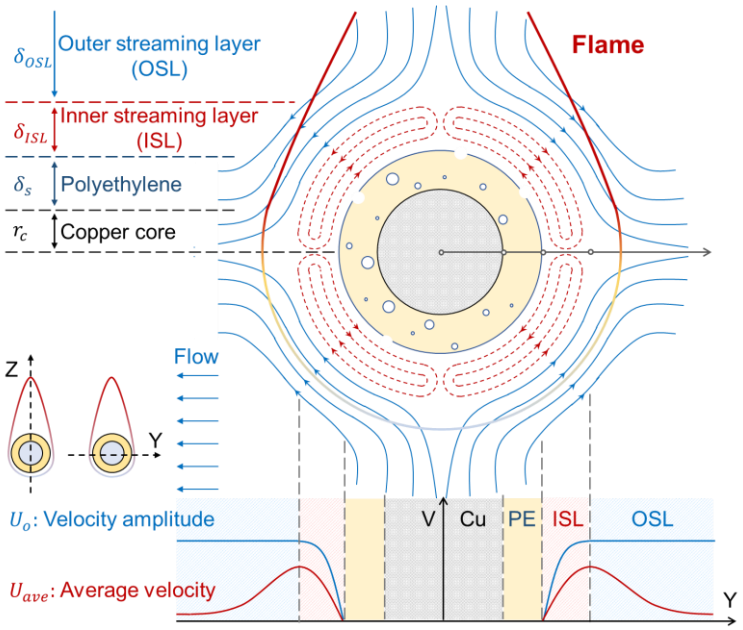

Fig. 6. Streamline of the oscillatory flow boundary around a burning wire.

The cross-sectional structure of the oscillatory boundary layer around the wire is detailed in Fig. 6. This configuration is corroborated by both experimental particle image velocimetry (PIV) measurement [29] and numerical simulation [30]. As can be seen, the near-surface region exhibits a two-layer structure, including 1) an inner streaming layer (ISL), generated by the viscous diffusion of vorticity on the cylinder surface [31], and 2) an outer streaming layer (OSL), located in the region radially further from the wire axis, produced by the balance between flow viscosity and its momentum diffusion on the wire surface [32]. Fig. 6 also shows that the air medium in ISL features close-loop streamlines with rotational motion, while the air in OSL displays counter-rotating vortices of larger spatial scales. Significantly, this dual-layer boundary persists even when thermally induced buoyancy effects are considered [23]. Hence, it still requires determining which type of boundary layer, ISL or OSL, plays a dominant role in the heat exchange between the flame and the fuel.

According to [31,32], the dynamics of both ISL and OSL boundaries are strongly dependent on oscillation condition, and their relative contributions to heat transfer can be quantified by an oscillating Reynolds number (Re_o):

$$Re_o = \frac{U_o^2}{\omega \gamma_g} \tag{2}$$

where U_o is the oscillating velocity amplitude, ω is the angular frequency, and γ_g is the gas-phase

kinetic viscosity. For a flow with Re_o < 75, the OSL will dominate the heat transfer process. Otherwise, it is necessary to consider the impact of ISL as a pure conduction layer [33]. In this work, U_o = 0.25 m/s, $\omega = 2\pi f_g$ = 314 s^{-1}, and γ_g = 76.4 × 10^{-6} m^2/s, leading to a maximum Reynolds number of around Re_o = 2.5. Hence, only the OSL-induced thermal boundary needs to be considered.

On the ground of the analysis above, the heat transfer under current oscillatory condition can be described by a mean oscillating Nusselt number ($\overline{Nu_o}$) [33]:

$$\overline{Nu_o} = 1.76(Pr{\cdot}Re_o)^{\frac{1}{2}}\left(1 + 0.83Pr^{\frac{1}{2}}\varphi/r_s\right) \tag{3}$$

where Pr = 0.72 is Prandtl number of air, $\varphi = U_o/\omega$ is the oscillatory amplitude, and r_s is the cylinder (wire) radius.

Worthy to note that there is no universal correlation to evaluate the oscillating velocity U_o required in Eq. (2). However, as measured in Fig. 4, $U_o = \epsilon U_{o,open}$, in which $U_{o,open}$ is experimentally measured to be close to the piston vibrating velocity (U_p), resulting in $U_o \cong \epsilon U_p$. Here, U_p can be further governed by both piston configuration and working states, so four parameters including piston vibrating pressure (P_p), frequency (f_p, equalling airflow oscillating frequency), piston radius (r_p) and its density (ρ_p) are identified to be the main factors to define U_p, given as:

$$U_p = \emptyset\left(P_p, f_p, r_p, \rho_p\right) \tag{4}$$

where the subscripts p denotes the piston device. By applying the Buckingham's Π theorem of dimensional analysis [34] to Eq. (4), one can obtain:

$$U_o = \epsilon U_p = C\frac{\epsilon P_p}{r_p \rho_p f_p} = C^*\frac{\epsilon P_p}{f_p} \tag{5}$$

where C^* = 2.1×10^{-2} m^2/kg, based on the fitting constants of C = 5.0, r_p = 0.2 m, and ρ_p = 1.2×10^3 kg/m^3.

E. Flame spreads in normal and oscillatory flows

Based on the above boundary analysis, the flame spread dynamics in oscillatory airflow can be mechanistically interpreted. Before extinction, the flame propagates continuously along the wire, transitioning through four distinct thermal zones, including a preheat region, a pyrolysis region, a bared core region, and a burnout region, see Fig. 7. To simplify the problem, several assumptions are adopted: 1) both the Cu core and PE insulation are thermally thin, 2) wire material properties are temperature-independent, 3) axial heat conduction within PE insulation is negligible, and 4) PE melting and phase change effects are excluded [15].

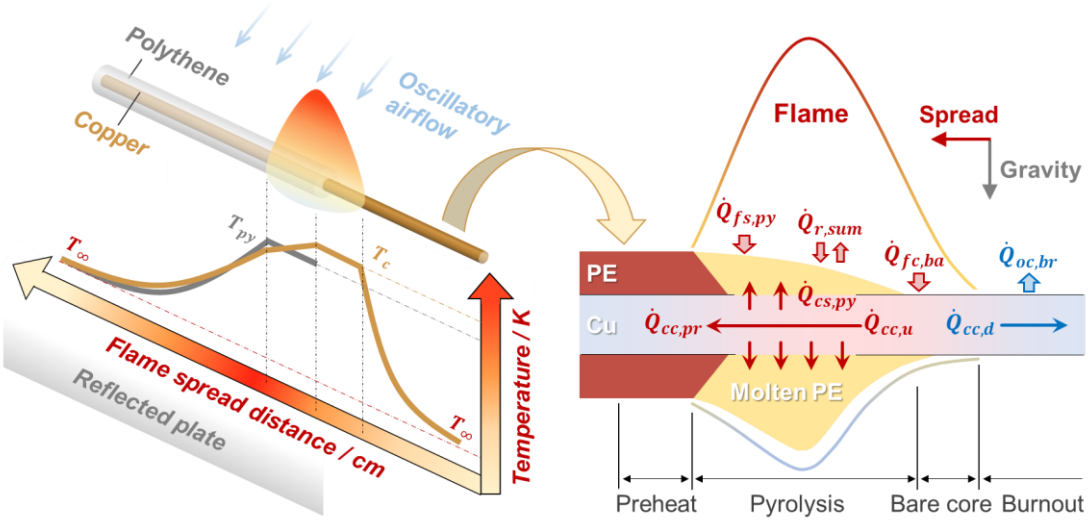

Fig. 7. Temperature distribution and heat transfer budgets in different regions of a horizontally burning wire.

Then, according to the conventional fire dynamics theory [35], FSR can be calculated as:

$$FSR = \frac{\dot{Q}_{r,sum} + \dot{Q}_{fc,ba} + \dot{Q}_{fs,py} - \dot{Q}_{oc,br}}{\rho_s A_s c_s\left[\left(T_{py} - T_\infty\right) + \left(\Delta H_{py}/C_s\right)\right] + \rho_c A_c c_c\left(T_{py} - T_\infty\right)} \tag{6}$$

where $\dot{Q}$, ρ, A, c, T, ΔH denote heat transfer rate, density, cross-section area, specific heat, temperature, and latent heat. The subscripts f, s, py, r, c, ba, o, br, ∞ denote flame, PE, pyrolysis, radiation, metal core, bare core, oscillatory airflow, burnt fuel, and ambient condition, respectively. For terms with combined subscripts, such as $\dot{Q}_{fs,py}$, this specifically denotes the heat transfer between flame (f) and PE (s) in pyrolysis region (py). In this work, latent heat of PE pyrolysis is set to ΔH_{py} = 254 kJ/kg [7].

In Eq. (6), the denominator quantifies the total thermal inertia of the wire, while the numerator accounts for various heat transfer mechanisms from the flame to the fuel. The first term in the numerator, $\dot{Q}_{r,sum}$, representing the radiative heating from the flame to the fuel when accounting for the re-radiation from the molten PE [36], is given as:

$$\dot{Q}_{r,sum} = \sigma L_{py}\left[\varepsilon_f d_s\left(T_f^4 - T_{py}^4\right) - \varepsilon_s G_s\left(T_{py}^4 - T_\infty^4\right)\right] \tag{7}$$

where σ, L_{py}, ε_f, ε_s, d_s, G_s are the Stefan-Boltzmann constant, pyrolysis region length, emissivities of flame and molten PE, wire diameter and perimeter. For other terms, T_f = 1200 K, T_{py} = 660 K, and T_∞ = 298 K denote the temperatures of flame, PE pyrolysis and surrounding environment.

The second term in the numerator of Eq. (6), $\dot{Q}_{fc,ba}$, which indicates the heat transfer between flame and Cu core in the bare-core region, can be calculated based on the heat balance within the core:

$$\dot{Q}_{fc,ba} = \dot{Q}_{cc,u} + \dot{Q}_{cc,d} \tag{8}$$

where $\dot{Q}_{cc,u}$ represents the total heat conduction from Cu core to different PE regions including its pyrolysis region $\dot{Q}_{cs,py}$ and preheat region $\dot{Q}_{cc,pr}$:

$$\dot{Q}_{cc,u} = \dot{Q}_{cs,py} + \dot{Q}_{cc,pr} = \frac{A_c \lambda_c \left(T_c - T_{py}\right)}{L_{py}} \tag{9}$$

where λ_c = 400 W/m-K is Cu conductivity and T_c (675-742 K) is the average temperature in the bare region. The other term in Eq. (8), $\dot{Q}_{cc,d}$, which represents another part of heat conduction from the Cu core to the burnout region, is considered equivalent to the convective cooling by oscillatory airflow ($\dot{Q}_{oc,br}$ in Eq. 6), based on the principle of heat balance as [13]:

$$\dot{Q}_{cc,d} \cong \dot{Q}_{oc,br} = (G_c A_c \lambda_c h_m)^{\frac{1}{2}}(T_c - T_\infty) \tag{10}$$

The third term in the numerator of Eq. (6) is $\dot{Q}_{fs,py}$, i.e., the convective heating from flame to PE insulation, expressed as:

$$\dot{Q}_{fs,py} \cong G_s L_{py} h_m (T_f - T_{py}) \tag{11}$$

Note that in Eqs. (10-11), a mixed heat transfer coefficient h_m is required, which is also the primary factor responsible for the difference in flame spread dynamics under oscillatory and steady airflows. In oscillatory conditions, h_m must both incorporate contributions from both buoyancy-induced natural convection and oscillation-induced forced convection, with the combined effects quantified by a mixed Nusselt number (Nu_m):

$$h_m = \frac{Nu_m \lambda_g}{d} \tag{12}$$

where λ_g = 5.4×10^{-2} W/m-K is air conductivity, d is the cylinder diameter, which varies depending on the wire regions: $d = d_c$ in the bare-core and burnout regions, and $d = d_s$ in the pyrolysis region. As recommended by [37], the mean Nu_m for a cylinder subjected to both natural and forced convections can be given as:

$$\overline{Nu}_m \cong (\overline{Nu}_N^4 + \overline{Nu}_F^4)^{\frac{1}{4}} \tag{13}$$

where $\overline{Nu}_N$ denotes the Nu number induced by natural convection, and $\overline{Nu}_F$ represents the Nu number induced by forced convection. For the former, $\overline{Nu}_N$, it can be expressed in terms of the Grashof number (Gr) and the Prandtl number as $\overline{Nu}_N = 0.85(Pr{\cdot}Gr)^{1/5}$, based on the typical fire-induced buoyant convection theory [37]. As for the forced Nu number, $\overline{Nu}_F$, it is clearly associated with the oscillatory airflow and can therefore be represented by the mean oscillating Nusselt number ($\overline{Nu}_o$) derived from the oscillatory boundary analysis in Eq. (3). Consequently, the mixed Nusselt number $\overline{Nu}_m$ in Eq. (13) can be calculated as:

$$\overline{Nu}_m \cong (\overline{Nu}_N^4 + \overline{Nu}_o^4)^{\frac{1}{4}} = \left(\frac{Pr^*}{\gamma_g f_g}\right)^{\frac{1}{2}} \left[\left(\frac{\gamma_g^* f_g}{Pr^{*\frac{3}{5}}}\right)^2 + U_o^4\right]^{\frac{1}{4}} = \left(\frac{Pr^*}{\gamma_g f_g}\right)^{\frac{1}{2}} U_m \tag{14}$$

where $Pr^* = 0.34$, U_m is the combined velocity at the flame position, resulting from the vector superposition of the vertical buoyant velocity and the horizontal RMS oscillatory velocity; $\gamma_g^* = \gamma_g^{1/5}(g\beta\Delta T d^3)^{2/5}$ is the effective viscosity of the fire plume, g = 9.8 m/s^2 is the gravitational acceleration, β = 3.66×10^{-3} K^{-1} is the volumetric thermal expansion coefficient, and ΔT = 900 K is the temperature difference between the flame and ambient air.

Upon substituting all terms from Eqs. (7–14) back into Eq. (6), the flame spread rate (FSR) over the electrical wire under oscillatory airflow can be quantified. Fig. 8 compares the theoretical prediction with experimental measurements across different oscillatory conditions. Notably, the model predictions based on Eq. (6) show excellent agreement with the experimental data, with a maximum error of less than 10 % in most tested scenarios. This slight deviation can be attributed to neglecting Marangoni convection and roughly replacing wire core temperature with PE pyrolysis temperature.

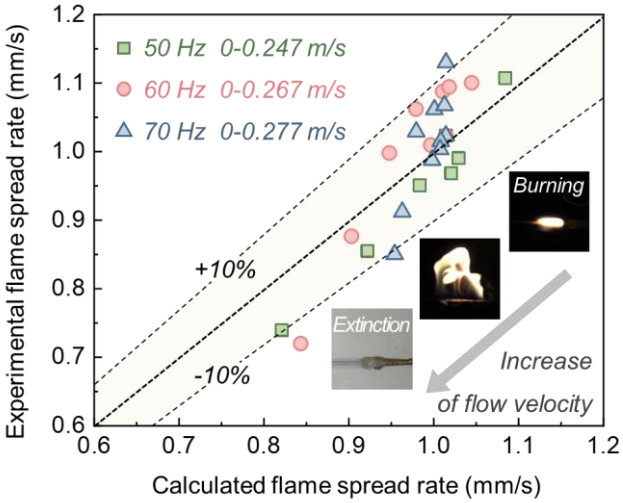

Fig. 8. Comparison of calculated and measured flame spread rate over wire under oscillatory airflow.

Based on accurate prediction of flame spread rate, the differences in the suppression capacities of oscillatory airflow and normal wind can be explained through heat transfer mechanisms. A 50-Hz airflow is taken as an example. Under such airflow, the flame spread rate and its heat transfer budgets calculated by Eq. (6) are plotted in Fig. 9a. For comparison, Fig. 9b presents analogous data under normal wind up to the blow-off condition. It is found that under the influence of both airflow patterns, the flame exhibits a similar behaviour, i.e., the flame spread becomes slower as the airflow velocity increases. It is also found that the convective heating from the flame to the fuel ($\dot{Q}_{fs,py} + \dot{Q}_{fc,ba}$) increases in both scenarios. This aligns with expectations, as this type of heat transfer typically increases with transverse airflow velocity due to the reduced flame-fuel distance [38].

The most prominent difference between Figs. 9a-b lies in the convective fuel cooling by external flow ($\dot{Q}_{oc,br}$) and the total radiative heating of the flame ($\dot{Q}_{r,sum}$). Notably, convective cooling effect ($\dot{Q}_{oc,br}$) exhibits considerably greater sensitivity to airflow velocity under oscillatory conditions. It can be seen that the gradient of $\dot{Q}_{oc,br}$ with respect to velocity in oscillatory airflow is about 2 times higher than that in steady wind, indicating a corresponding enhancement in the convective heat transfer coefficient for oscillatory flow regimes. Additionally, flame radiative heating ($\dot{Q}_{r,sum}$) demonstrates accelerated decay under oscillatory conditions. For instance, reducing $\dot{Q}_{r,sum}$ from an initial 6.53 W to 4.66 W requires only 0.10 m/s oscillatory airflow velocity, whereas a 0.47 m/s velocity is required for steady wind. This suggests a greater suppression efficacy of oscillatory airflow on flame intensity,

primarily attributed to enhanced flame stretching and temperature attenuation.

Worthy to note that while this study focuses specifically on PE cables, the fuel properties such as pyrolysis temperature (T_{py}), heat capacity (c_s), and emissivity (ε_s) are integrated into Eqs. (6–9). Hence, for other types of fuels, the influence of their property variations on the extinction process can be qualitatively analysed. For instance, as T_{py} increases, the numerator of Eqs. (6) decreases while its denominator increases, resulting in a smaller FSR value that facilitates extinction. Likewise, an increase in either c_s or ε_s can also promote extinction.

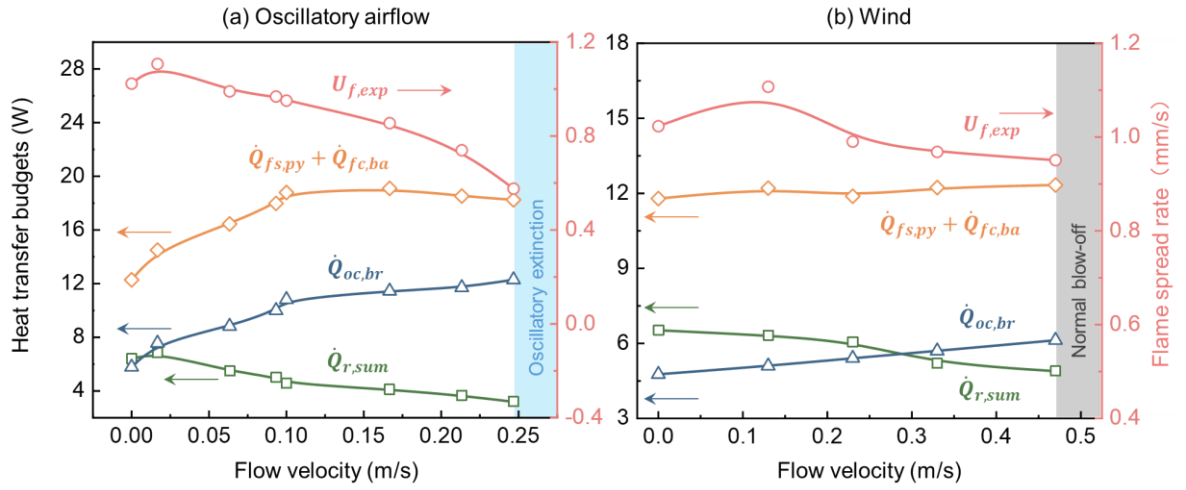

Fig. 9. Comparison of flame spread rate and heat transfer budgets under (a) 50-Hz oscillatory airflow and (b) normal wind conditions.

F. Oscillation-induced unsteady effects

It is still required to examine the superior extinguishing performance of low-frequency airflow. Beyond heat transfer analysis, airflow-induced extinction can also be interpreted within the framework of flame morphology, specifically the stretching state of the flame sheet. For extinctions induced by steady wind, the extinction flame strain rate is widely regarded as a stable indicator of extinction limits [11]. As for oscillatory airflow-induced extinctions, the strain rate of flame over cylindrical electrical wire can be defined as [39]:

$$a_m = \frac{2U_m}{r_s} = \frac{2\left[\left(\gamma_g^* f_g / Pr^{*\frac{3}{5}}\right)^2 + U_o^4\right]^{\frac{1}{4}}}{r_s} \tag{15}$$

where U_m denotes the resultant velocity vectors combining transverse oscillatory velocity and vertical fire-induced buoyant velocity, and r_s denotes the wire radius.

Solutions of Eq. (15) at extinction limits across oscillating frequencies from 50-70 Hz are plotted in Fig. 10a. As can be seen, the strain rate of flames subjected to oscillatory airflow is not constant but varies with oscillating frequency and velocity. This is consistent with exceptions, as the inherently laminar flame structure will transition to a turbulent process under oscillatory excitation. Hence, the

results presented in Fig. 10a are, in fact, a typical feature of turbulent flow, where the characteristic flame motion is proportional to the strain field [40]. Therefore, the unsteady effects originating from the timescale competition between external perturbation and flame diffusion [40], which are responsible for faster flame extinction under an elevated strain field, requires a detailed examination.

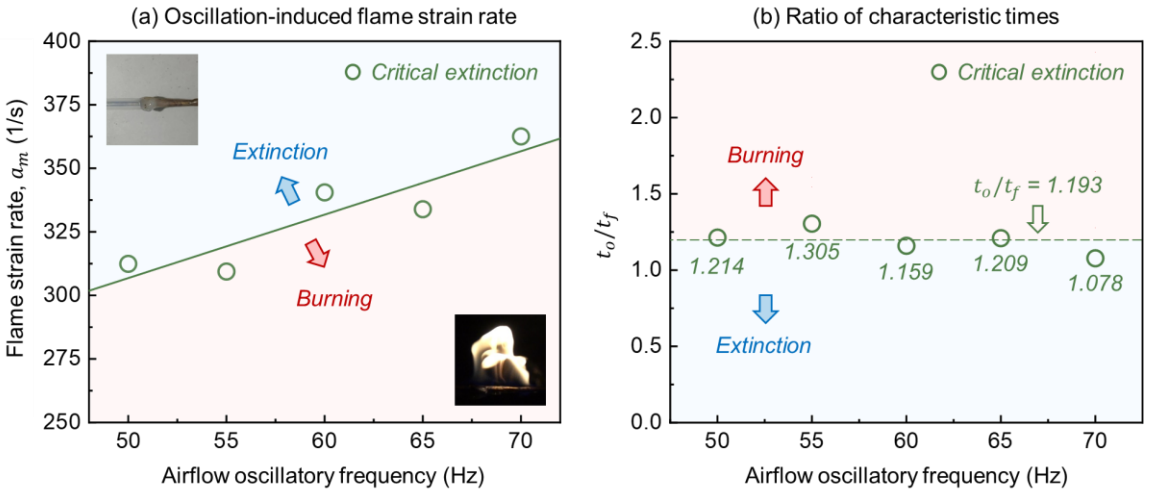

Fig. 10. Dependences of (a) flame strain rate and (b) t_o/t_f on airflow oscillatory frequency at extinction limits.

Based on conventional turbulent combustion theory, when the characteristic timescale of external perturbation is comparable to those of flame diffusion and reaction [41], steady-state analyses become inappropriate, and unsteady effects must be considered [42]. In this work, the external perturbation time (t_o) is defined as one quarter of the airflow oscillation period, given by $t_o = \varphi_g/U_o$, where φ_g and U_o represent air oscillation amplitude and velocity, respectively. The flame diffusion time can be calculated as the time required for pyrolysis gas to diffuse to the flame surface [35], i.e., $t_f = \delta_f^2/D_g$, where δ_f = 1 mm is the flame thickness [40] and D_g = 4.0×10^{-5} m^2/s is the diffusivity of polymer vapor [43]. A comparison of these two timescales at different extinction limits is given in Fig. 10b. As shown, the ratio of t_o/t_f remains close to 1 across varying frequencies, indicating that unsteady effects indeed play a critical role in oscillation-induced flame extinction.

According to [40], the unsteady effects can be described by a hyperbolic curve as:

$$(a_m - a_m^0)(t_o - t_o^0) = C_1 \tag{16}$$

where a_m and t_o are the measured extinction strain rate and perturbation time, respectively, and C_1 is a fitting constant. The other two terms in Eq. (16), a_m^0 and t_o^0, correspond to the asymptotes of the hyperbola and represent two idealized limits of the extinction process. For a slowly oscillating airflow with an oscillation period approaching infinity, its perturbation time t_o can be very large. In such condition, the extinction strain rate a_m will approach to a critical value a_m^0, which corresponds to the quasi-steady extinction strain rate of a pure diffusion flame sheet. Conversely, for an ultra-fast oscillating airflow where the perturbation time t_o falls below the threshold t_o^0, there is insufficient time for flame diffusion to respond before the airflow passes through, and thereby no extinction occurs.

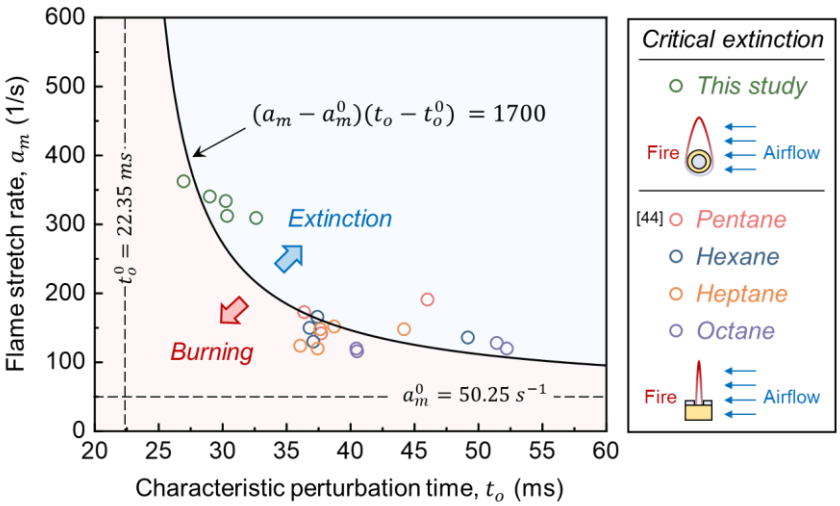

Fig. 11. The extinction strain rate (a_m) as a function of airflow perturbation time (t_o).

In Fig. 11, the measured strain rate a_m is plotted as a function of the perturbation time t_o at different extinction limits for various fire configurations [44]. As can be seen, a hyperbolic correlation indeed exists between these two parameters, with the best fitted curve to be drawn with a constant of C_1 = 1700. As seen, the horizontal asymptote approaches a_m^0 = 50.25 s^{-1}, which is close to the theoretical prediction from an idealized Tsuji-burner diffusion flame [39]. It is also observed that the vertical asymptote approaches t_o^0 = 22.35 ms, indicating that the flame over electrical wire acts as a low-pass filter with completely no response to the airflows oscillating at frequencies higher about 180 Hz (≈ 4×1000 ms/22.14 ms). This observation is corroborated by existing combustion studies [40,45], where high-frequency external perturbations (such as the inflow excitation for gas burner [46]), are frequently employed to enhance combustion efficiency rather than impede the reaction process.

G. Extinction criterion

Given that convective fuel cooling and unsteady flame stretch may jointly contribute to extinctions caused by oscillatory airflow, it is theoretically feasible to develop a criterion integrating both effects for accurately determining the extinction limits. The unsteady effect can be simply quantified using the flame strain rate (a_m). The fuel cooling effect, on the other hand, can be characterized by a heat loss factor (Θ), which estimates the relative magnitude of fuel heat loss compared to the total heat input from the flame to the fuel. Specifically, the heat loss primarily involves the convective fuel cooling due to oscillatory airflow ($\dot{Q}_{oc,br}$), while the total heat input includes both flame radiative heating ($\dot{Q}_{r,sum}$) and convective heating effects ($\dot{Q}_{fc,ba} + \dot{Q}_{fs,py}$). Therefore, Θ is expressed as:

$$\Theta = \left| \frac{\dot{Q}_{oc,br}}{\dot{Q}_{fs,py} + \dot{Q}_{fc,ba} + \dot{Q}_{r,sum}} \right| \tag{17}$$

Fig. 12a illustrates the variation of Θ with a_m across different cases encompassing successful and failed extinctions. As seen, the heat loss factor Θ exhibits a linear correlation with the unsteady flame

stretch rate a_m, which can be described as:

$$\Theta \cdot a_m = C_2 \tag{18}$$

where C_2 = 178.8 is a fitting constant obtained for the best fitted curve. Above this curve, oscillatory airflow-induced extinction becomes inevitable. Conversely, below this curve, the flame will continue to spread along the wire and no extinction will occur.

To further confirm that Eq. (18) can serve as a universal extinction indicator for other wires subjected to airflow disturbance, additional data obtained from steady wind-induced extinctions [7] of various wire configurations are presented in Fig. 12b. These data are calculated by substituting steady Nusselt number and airflow velocity into Eqs. (15) and (17). It can be seen in Fig. 12b that all the circular scatters display a consistent trend of variation, indicating that Eq. (18) can be a robust criterion for identifying the extinction limits, regardless of whether oscillatory or steady airflow is used to suppress wire fire hazards in confined environments. Note that the proposed criterion is only applicable to wires with a Cu core. For other core materials such as NiCr, the prediction error may exceed 20%. Hence, further research is still needed for an improved extinction criterion.

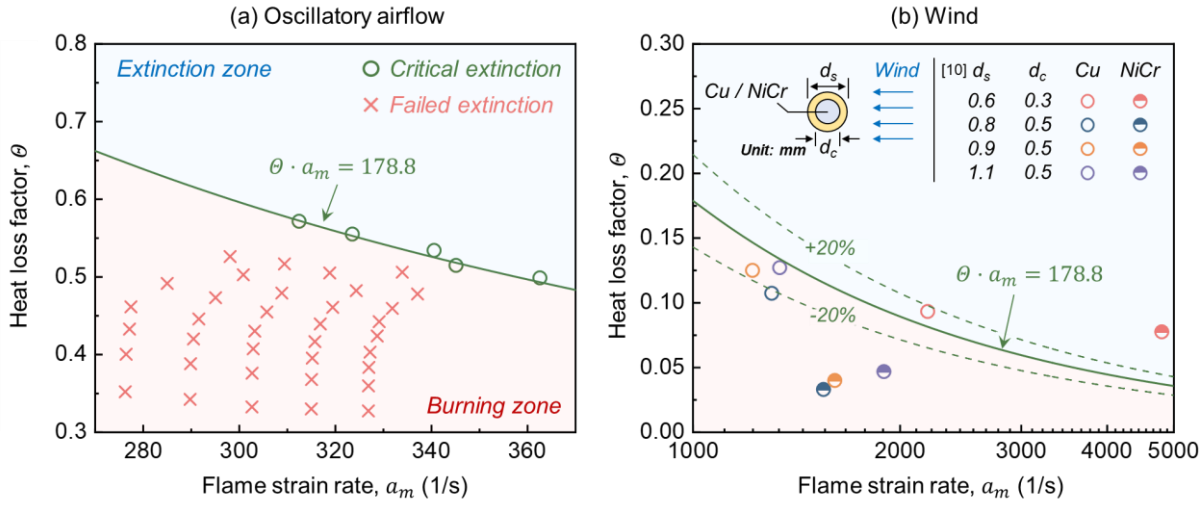

Fig. 12. Correlation between heat loss (Θ) and flame strain rate (a_m) under (a) oscillatory airflow and (b) normal wind across various extinction limits.

IV. Conclusions

This work proposes a firefighting method that employs oscillatory airflow to suppress wire fire hazards in confined environments. The extinguishing target selects a 100 mm-long wire with a diameter of 4 mm, featuring PE insulation and a Cu core. During experiments, the wire is horizontally placed, and its flame is transversely exposed to external airflow disturbance. An electromagnetic piston system is developed to generate oscillatory airflows, with the oscillation frequency ranging from 50-70 Hz and the RMS velocity varying below 0.28 m/s. For comparison, the typical blow-off caused by a fan system at the same velocity is also tested.

Results show that, compared with steady wind, oscillatory airflow can achieve the extinction of

wire flames in confined spaces at a lower airflow velocity and with reduced energy consumption. In particular, the lower the oscillation frequency used, the lower the required airflow energy for extinction. To examine the underlying mechanism, the heat transfer between the flame and the fuel is analyzed, combined with the analysis of the oscillation-induced heat exchange boundary near the wire surface. Two factors are found to contribute to the performance of the oscillatory airflow: 1) convective fuel cooling by oscillatory airflow is about 2 times higher than that by steady wind, and 2) radiative heating from the flame to the fuel is greatly weakened due to a lower flame temperature in oscillatory flows.

The superior performance of low-frequency airflow is further examined by analyzing the unsteady effects of the flame sheet during the extinction process. It is found that the current wire configuration could act as a low-pass filter and show resistance to responding to airflows oscillating at frequencies higher than about 180 Hz, caused by the comparable timescales of flame diffusion and external airflow perturbation near the extinction limits. On the ground of this, a criterion coupling wire heat loss and airflow perturbation is established to accurately identify the critical extinction condition. This work proposes a low-carbon firefighting technique that utilizes normal air as the extinguishing agent, and it helps expand the design channels of fire safety and firefighting systems in constrained spaces. Still, future research is required to reveal impacts such as wire electrification and flame spread orientation.

Acknowledgments

C. X. is supported by the Science and Technology Program of Guangzhou, China (2024A04J3263) and the Natural Science Foundation of Guangdong Province (2024A1515012261); J. Z. is funded by the National Natural Science Foundation of China (22408108); X. H. is funded by the Hong Kong Research Grants Council Theme-based Research Scheme (T22-505/19-N).

Reference

[1] M. Ahrens, Home Structure Fire (National Fire Protection Association, Fire Analysis and Research Division, 2013).

[2] N.N. Bakhman, L.I. Aldabaev, B.N. Kondrikov, and V.A. Filippov, “Burning of polymeric coatings on copper wires and glass threads: I. Flame propagation velocity,” Combust. Flame **41**, 17–34 (1981).

[3] Y. Chen, J. Jia, X. Liu, and W. Shen, “Impact of sealing speeds on the mechanism of hot smoke propagation in tunnel fires under single-sided and double-sided sealing conditions,” Phys. Fluids **37**(3), (2025).

[4] Y. Chen, W. Shen, and J. Jia, “Influence mechanism of longitudinal ventilation and bifurcation angle on tunnel fire temperature distribution and smoke diffusion,” Phys. Fluids **37**(4), (2025).

[5] H. Du, Z. Tang, S. Meng, and D. Zhou, “Tunnel shaft impact on smoke transport in fire-induced high-speed train stopping,” Phys. Fluids **37**(2), (2025).

[6] X. Huang, and Y. Nakamura, “A Review of Fundamental Combustion Phenomena in Wire Fires,” Fire Technol. **56**(1), 315–360 (2020).

[7] Y. Ma, X. Zhang, Y. Lu, J. Lv, N. Zhu, and L. Hu, “Effect of transverse flow on flame spread and extinction over polyethylene-insulated wires,” Proc. Combust. Inst. **38**(3), 4727–4735 (2021).

[8] Y. Lu, X. Huang, L. Hu, and C. Fernandez-Pello, “Concurrent Flame Spread and Blow-Off Over

Horizontal Thin Electrical Wires," Fire Technol. **55**(1), 193–209 (2019).
[9] S. Jia, L. Hu, Y. Ma, X. Zhang, and O. Fujita, "Experimental study of downward flame spread and extinction over inclined electrical wire under horizontal wind," Combust. Flame **237**(3), 111820 (2022).
[10] Y. NAKAMURA, N. YOSHIMURA, T. MATSUMURA, H. ITO, and O. FUJITA, "Opposed-wind Effect on Flame Spread of Electric Wire in Sub-atmospheric Pressure," J. Therm. Sci. Technol. **3**(3), 430–441 (2008).
[11] Y. Lu, X. Huang, L. Hu, and C. Fernandez-Pello, "The interaction between fuel inclination and horizontal wind: Experimental study using thin wire," Proc. Combust. Inst. **37**(3), 3809–3816 (2019).
[12] L. Zhao, Q. Zhang, R. Tu, J. Fang, J. Wang, and Y. Zhang, "Effects of electric current and sample orientation on flame spread over electrical wires," Fire Saf. J. **112**, 102967 (2020).
[13] Y. Konno, N. Hashimoto, and O. Fujita, "Downward flame spreading over electric wire under various oxygen concentrations," Proc. Combust. Inst. **37**(3), 3817–3824 (2019).
[14] Y. Konno, N. Hashimoto, and O. Fujita, "Role of wire core in extinction of opposed flame spread over thin electric wires," Combust. Flame **220**, 7–15 (2020).
[15] Y. Kobayashi, Y. Konno, X. Huang, S. Nakaya, M. Tsue, N. Hashimoto, O. Fujita, and C. Fernandez-Pello, "Effect of insulation melting and dripping on opposed flame spread over laboratory simulated electrical wires," Fire Saf. J. **95**, 1–10 (2018).
[16] S. Jia, Y. Ma, Z. Guo, and L. Hu, "Experimental study of spontaneous ignition of overloaded electrical wires under transverse wind," Proc. Combust. Inst. **39**(3), 4031–4039 (2023).
[17] J.M. Valverde, "Pattern-formation under acoustic driving forces," Contemp. Phys. **56** (2015).
[18] S. Komarov, and M. Hirasawa, "Enhancement of gas phase heat transfer by acoustic field application," Ultrasonics **41**(4), 289–293 (2003).
[19] A. Gopinath, and D.R. Harder, "An experimental study of heat transfer from a cylinder in low-amplitude zero-mean oscillatory flows," Int. J. Heat Mass Transf. **43**(4), 505–520 (2000).
[20] J.W. Bennewitz, D. Valentini, M.A. Plascencia, A. Vargas, H.S. Sim, B. Lopez, O.I. Smith, and A.R. Karagozian, "Periodic partial extinction in acoustically coupled fuel droplet combustion," Combust. Flame **189**, 46–61 (2018).
[21] J.S. Kim, and F.A. Williams, "Contribution of strained diffusion flames to acoustic pressure response," Combust. Flame **98**(3), 279–299 (1994).
[22] D.J. McKINNEY, and D. DUNN-RANKIN, "Acoustically Driven Extinction in a Droplet Stream Flame," Combust. Sci. Technol. **161**(1), 27–48 (2000).
[23] F.M. Mahfouz, and H.M. Badr, "Mixed convection from a cylinder oscillating vertically in a quiescent fluid," Heat Mass Transf. **38**(6), 477–486 (2002).
[24] S. Yesilyurt, M. Ozcan, and G. Goktug, "Heat Transfer in Steady-Periodic Flows over Heated Microwires," in Forced Convect., (Begell House Inc., 2006).
[25] B.J. Davidson, "Heat transfer from a vibrating circular cylinder," Int. J. Heat Mass Transf. **16**(9), 1703–1727 (1973).
[26] G. shan Jiang, Y. feng Yang, W. long Xu, M. Yu, and Y. chao Liu, "Convective heat exchange characteristics of acoustic-induced flows over a sphere: The role of acoustic streaming," Appl. Acoust. **177**, 107915 (2021).
[27] J. Eargle, Loudspeaker Handbook (Springer Science & Business Media, 2003).
[28] H.Schlichting, "Berechnung ebener periodischer Grenzschichtstromungen," Phys. Zeit **33**, 327–335

(1932).

[29] E.N.D.C.Andrade, "On the circulations caused by the vibration of air in a tube," Proc. R. Soc. London. Ser. A, Contain. Pap. a Math. Phys. Character **134**(824), 445–470 (1931).

[30] Y. Liu, G. Jiang, Y. Yang, Q. Kong, and Y. Jiang, "Numerical simulation on acoustic streaming characteristics in boiler tube array," Int. J. Heat Mass Transf. **193**, 122834 (2022).

[31] J.T. Stuart, "Double boundary layers in oscillatory viscous flow," J. Fluid Mech. **24**(04), 673 (1966).

[32] C.P. Lee, and T.G. Wang, "Outer acoustic streaming," J. Acoust. Soc. Am. **88**(5), 2367–2375 (1990).

[33] P.D. Richardson, "Heat transfer from a circular cylinder by acoustic streaming," J. Fluid Mech. **30**(2), 337–355 (1967).

[34] E. Buckingham, "On Physically Similar Systems; Illustrations of the Use of Dimensional Equations," Phys. Rev. **4**(4), 345–376 (1914).

[35] Drysdale D, An Introduction to Fire Dynamics (John wiley & sons, 2011).

[36] X. Huang, Z. Zhou, J. Hu, M. Zhang, Y. Zhang, H. Zhu, C. Liu, and P. Zhang, "Research on flame spread and combustion characteristics of double parallel PE wires under different currents and spacing distances," Therm. Sci. Eng. Prog. **43**, 102001 (2023).

[37] F.P. Incropera, and D.P. DeWitt, Fundamentals of Heat and Mass Transfer (New York: Wiley, 1996).

[38] Y. Ma, X. Sun, Z. Guo, Y. Gu, O. Fujita, and L. Hu, "Flame extinction over electrical wires under transverse flow: Critical damkohler number analysis incorporating solid-phase heat conduction," Energy **315**, 134278 (2025).

[39] H. Tsuji, and I. Yamaoka, "Structure and extinction of near-limit flames in a stagnation flow," Symp. Combust. **19**(1), 1533–1540 (1982).

[40] A. Lemaire, K. Zähringer, T.R. Meyer, and J.C. Rolon, "Unsteady effects on flame extinction limits during gaseous and two-phase flame/vortex interactions," Proc. Combust. Inst. **30**(1), 475–483 (2005).

[41] Peters N., Turbulent Combustion (Cambridge, UK: Cambridge University Press, 2000).

[42] D.C. Haworth, M.C. Drake, S.B. Pope, and R.J. Blint, "The importance of time-dependent flame structures in stretched laminar flamelet models for turbulent jet diffusion flames," Symp. Combust. **22**(1), 589–597 (1989).

[43] Holman J., Heat Transfer, tenth edit (McGraw Hill Higher Education, 2009).

[44] A.N. Friedman, and S.I. Stoliarov, "Acoustic extinction of laminar line-flames," Fire Saf. J. **93**, 102–113 (2017).

[45] T.M. Brown, R.W. Pitz, and C.J. Sung, "Oscillatory stretch effects on the structure and extinction of counterflow diffusion flames," Symp. Combust. **27**(1), 703–710 (1998).

[46] D. Mejia, M. Miguel-Brebion, A. Ghani, T. Kaiser, F. Duchaine, L. Selle, and T. Poinsot, "Influence of flame-holder temperature on the acoustic flame transfer functions of a laminar flame," Combust. Flame **188**, 5–12 (2018).